Carbonate mineral saturation states along the U.S. East Coast

Li-Qing Jiang,[a],[*],[1] Wei-Jun Cai,[a] Richard A. Feely,[b] Yongchen Wang,[a] Xianghui Guo,[a],[2] Dwight K. Gledhill,[c] Xinping Hu,[a] Felipe Arzayus,[d] Feizhou Chen,[a],[3] Justin Hartmann,[a] and Longjun Zhang[e]

[a] Department of Marine Sciences, University of Georgia, Athens, Georgia
[b] Pacific Marine Environmental Laboratory, National Oceanic and Atmospheric Administration, Seattle, Washington
[c] Cooperative Institute of Marine and Atmospheric Studies, Rosenstiel School, Marine Biology and Fisheries, University of Miami, Miami, Florida; Atlantic Oceanographic and Meteorological Laboratory, National Oceanic and Atmospheric Administration, Miami, Florida
[d] Office of Ocean Exploration and Research, National Oceanic and Atmospheric Administration, Silver Spring, Maryland
[e] College of Environmental Science and Engineering, Ocean University of China, Qingdao, Shandong Province, China

Abstract

To assess the impact of ocean acidification on the carbonate chemistry of the shelf waters off the southeastern United States (South Atlantic Bight [SAB]), we measured carbonate mineral saturation states from January 2005 to May 2006. The findings reveal that aragonite (Ω_{arag}: 2.6–4.0) and calcite (Ω_{cal}: 4.1–6.0) saturation states were considerably higher than those recently reported along the West Coast of North America. Different water mass age between the Atlantic and Pacific Oceans during global ocean circulation is the primary reason for the higher carbonate mineral saturation states in the SAB than along the West Coast. The contrasting water temperatures in the two coasts contribute to such differences. Both upwelling and freshwater discharge also play important roles in controlling saturation state. Carbonate mineral saturation in the surface water of the West Coast is strongly controlled by the upwelling of high-salinity, low-temperature, low-oxygen, and low-pH deep water. In comparison, saturation states in the surface water of the SAB coast are rarely affected by upwelling. Instead, they are strongly influenced by the input of low-saturation-state water from rivers. Continued increases of atmospheric CO_2 under the Intergovernmental Panel on Climate Change B1 emission scenario will decrease the carbonate mineral saturation states by up to 40% by the end of this century, and aragonite will approach undersaturation near the coast.

Over the last 2 million yr, atmospheric concentrations of CO_2 oscillated between 160 and 300 $\mu mol\ mol^{-1}$ (or parts per million in volume), as Earth cycled from glacial to interglacial periods (Hönisch et al. 2009). Since the start of the industrial revolution, human activities, including the burning of fossil fuels, land use changes, and cement production, have released more than 540 billion tons of CO_2 into the atmosphere (Marland et al. 2009). As a result, atmospheric CO_2 has increased by nearly 40% to 390 $\mu mol\ mol^{-1}$ today and is expected to approach 800 $\mu mol\ mol^{-1}$ by the end of this century, assuming the Intergovernmental Panel on Climate Change (IPCC) B1 emission scenario (Nakićenović and Swart 2000).

The rapidly increasing CO_2 in the atmosphere is expected to bring about pronounced changes in our climate system. However, climate change is not the only problem caused by the increase of atmospheric CO_2. Every year, ~ 30% of all the CO_2 that is released by human activities is taken up by the world's oceans (Le Quéré et al. 2009). This process comes with geochemical consequences for the global oceans. Through the uptake of CO_2, the upper oceans undergo considerable change in carbonate chemistry in a process commonly referred to as ocean acidification (Caldeira and Wickett 2003; Feely et al. 2004; Orr et al. 2005).

As CO_2 reacts with water, it forms carbonic acid (H_2CO_3), which rapidly disassociates, generating hydrogen ions (H^+), thereby lowering pH (hence the term ocean acidification). In seawater, this reaction is buffered whereby H^+ combines with carbonate ion (CO_3^{2-}) to form bicarbonate ion (HCO_3^-). Therefore, the overall reaction results in a decrease in pH and CO_3^{2-} ion concentration (Feely et al. 2004; Orr et al. 2005; Doney et al. 2009b). The decline in carbonate ion has a corresponding effect on the degree to which seawater is saturated with respect to the carbonate minerals (e.g., aragonite, calcite, magnesian calcite) that compose many shallow-water marine sediments and are formed by many marine organisms to construct their shells (Doney et al. 2009a).

Carbonate mineral saturation state is defined according to:

$$\Omega = \frac{[Ca^{2+}][CO_3^{2-}]}{K_{sp}} \quad (1)$$

where Ω is the saturation state ($\Omega > 1$ favors precipitation and $\Omega < 1$ favors dissolution), $[Ca^{2+}]$ and $[CO_3^{2-}]$ are the concentrations of calcium and carbonate ion, respectively, and K_{sp} is the stoichiometric solubility product that is

* Corresponding author: Liqing.Jiang@yale.edu

Present addresses:
[1] Yale School of Forestry & Environmental Studies, Yale University, New Haven, Connecticut
[2] Research Center for Environmental Changes, Academia Sinica, Nankang, Taipei, Taiwan
[3] Department of Oceanography, Dalhousie University, Halifax, Nova Scotia, Canada

Table 1. Carbonate mineral saturation states in the surface water (area-averaged) of the inner, middle, and outer shelves during all sampling months and the year 2100.

	Aragonite (Calcite)					
	Jan 2005	Mar 2005	May 2006	Jul 2005	Oct 2005	Dec 2005
Current						
Inner	3.0 (4.7)	2.6 (4.1)	3.3 (5.0)	3.6 (5.4)	3.1 (4.6)	2.9 (4.5)
Middle	3.5 (5.3)	3.3 (5.1)	3.5 (5.4)	3.9 (5.8)	3.7 (5.6)	3.5 (5.4)
Outer	3.9 (5.9)	3.7 (5.7)	3.8 (5.7)	4.0 (5.9)	4.0 (6.0)	3.8 (5.8)
2100	Jan	Mar	May	Jul	Oct	Dec
Inner	1.8 (2.8)	1.6 (2.5)	2.4 (3.7)	3.0 (4.4)	2.5 (3.7)	1.7 (2.6)
Middle	2.2 (3.3)	2.0 (3.1)	2.5 (3.9)	3.1 (4.6)	2.7 (4.1)	2.1 (3.3)
Outer	2.5 (3.8)	2.3 (3.6)	2.7 (4.0)	3.1 (4.6)	2.9 (4.3)	2.5 (3.8)

mainly dependent on pressure, temperature, and salinity. K_{sp} is either defined for aragonite or calcite (aragonite is more soluble than calcite), two common mineral phases of calcium carbonate ($CaCO_3$) secreted by marine organisms.

According to data and emission scenarios available for the last 2 centuries, saturation states of aragonite and calcite had declined $\sim$ 16% from preindustrial values by the year 2000 and are expected to decrease to $\sim$ 50% of preindustrial values by 2100 (Wolf-Gladrow et al. 1999; Kleypas et al. 2006; Feely et al. 2009). A reduction in saturation states has been experimentally determined to affect the ability of many marine organisms to form their shells and skeleton structure (Kleypas et al. 1999; Fabry 2008; Ries et al. 2009). In addition, ocean acidification is

changing the physical (Brewer and Hester 2009) and chemical properties of seawater (Millero et al. 2009) and rates of many biogeochemical processes in the ocean (Hutchins et al. 2009).

Understanding ocean acidification in the coastal ocean is particularly important, considering that many commercial fisheries and potentially sensitive calcifying marine species including mollusks (oysters and clams) and crustaceans (shrimp and blue crabs) are located in these regions. Waters corrosive to some forms of shelled marine organisms and sediments (aragonite saturation state: $\Omega_{arag} < 1$) have been detected during upwelling along the West Coast of North America (Feely et al. 2008). However, few surveys have examined the distribution of carbonate mineral saturation states along the East Coast of North America.
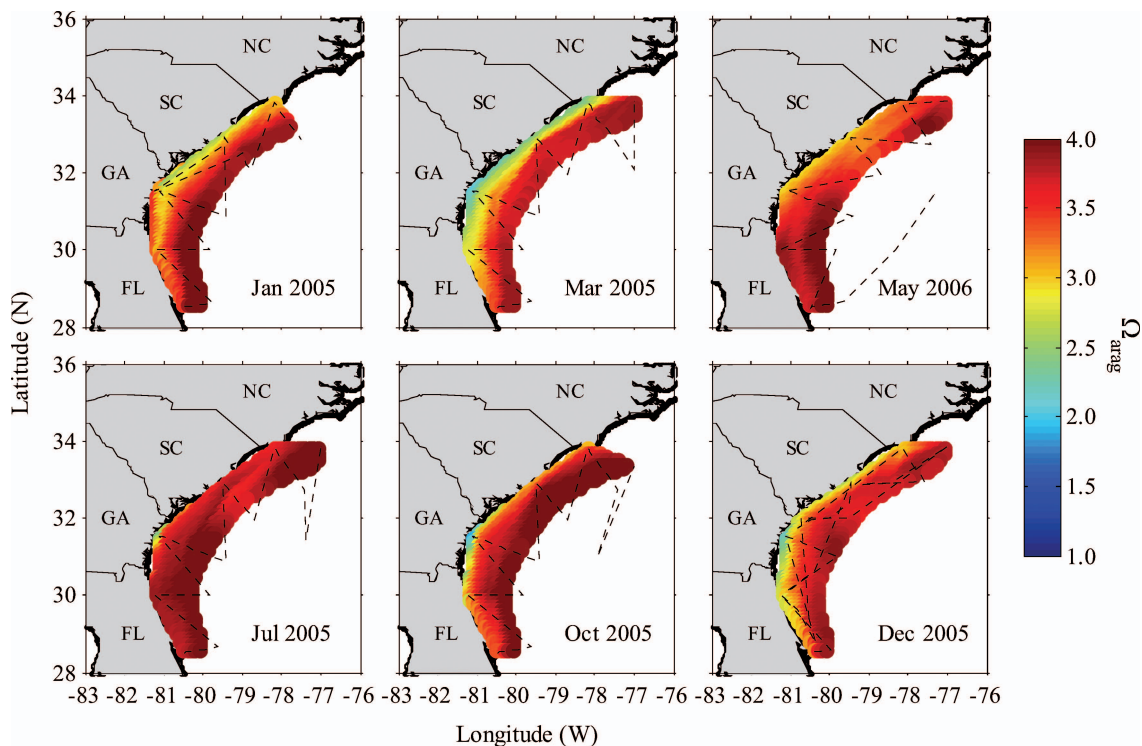

Fig. 1. Spatial distributions of surface water aragonite saturation state (Ω_{arag}) during all sampling months in the SAB. The dotted lines show the ship track on which the interpolation is based. NC, North Carolina; SC, South Carolina; GA, Georgia; FL, Florida.

Because of the younger water mass age and less accumulation of respired CO_2 as ocean circulates along the conveyor belt, the Atlantic Ocean features much higher carbonate mineral saturation states relative to the Pacific Ocean (Broecker 2003; Feely et al. 2004). It is thus expected that the challenge posed by ocean acidification within the East Coast of North America is less serious than that in the West Coast. In this study, aragonite and calcite saturation states were surveyed along the continental shelf of the southeastern United States from January 2005 to May 2006. Processes controlling the saturation states are discussed. Future effects of anthropogenic CO_2 on the saturation states are also explored.

Methods

Study site—The southeastern U.S. continental shelf, also known as South Atlantic Bight (SAB), extends along the eastern U.S. coast from Cape Hatteras, North Carolina to West Palm Beach, Florida. The shallow coastal water spreads out to the shelf break where the water depth is around 50–75 m. The northward-flowing Gulf Stream runs along the shelf break. There are extensive salt marshes lying off the coastline of Georgia and South Carolina. Most rivers in this region are located in the central and northern part of the shelf. River discharge usually peaks in February–April and has minimum flow in September–November, with a total annual discharge of about 66 km³ ($\sim$ 2.7% of the SAB volume).

Field measurements—Six cruises, 05–16 January 2005, 19–30 March 2005, 27 July–05 August 2005, 07–17 October 2005, 16–21 December 2005, and 17–27 May 2006, were conducted to map the distribution of aragonite and calcite saturation states across the region. The vertical sample spacing was designed to sample depth intervals as close as 10 m around the surface and gradually increase as depth increases.

pH was measured onboard the research vessel on the basis of a spectrophotometric pH method (Clayton and Bryne 1993). Samples for pH were kept in a water bath with a constant temperature of 25°C for $\sim$ 30 min before the measurement. Samples for dissolved inorganic carbon (DIC) were preserved with $HgCl_2$ and stored in a refrigerator on board the research vessel. DIC was determined with an automated DIC analyzer within a week after each cruise (Cai and Wang 1998). In May 2006, dissolved oxygen (DO) concentrations were determined using a spectrophotometric Winkler method (Pai et al. 1993).

Derivation of carbonate mineral saturation states—Carbonate mineral saturation states were calculated on the basis of Eq. 1. Carbonate ion concentration ($[CO_3^{2-}]$) was calculated from DIC and pH using a Matlab version (van Heuven et al. 2009) of the CO2SYS program (Lewis and Wallace 1998). For the calculation, the dissociation constants for carbonic acid of Mehrbach et al. (1973) as refit by Dickson and Millero (1987) and for $KHSO_4^-$ of Dickson (1990) were used. The concentration of calcium ($[Ca^{2+}]$) was calculated from salinity according to Riley and

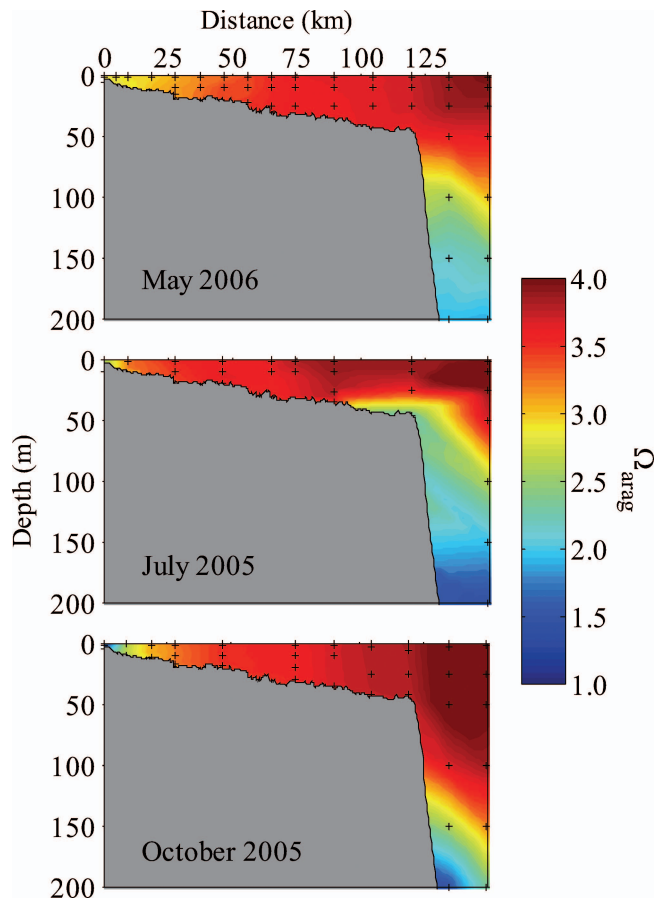Fig. 2. Vertical distributions of aragonite saturation state (Ω_{arag}) on C-transect of the SAB (Jiang et al. 2008) in May 2006, July 2005, and October 2005. The pluses show the sampling depths on which the interpolation is based.

Tongudai (1967). K_{sp} of aragonite and calcite were calculated on the basis of Mucci (1983).

Results

The SAB coast was supersaturated with respect to aragonite (as well as calcite, which will be discussed later) in all sampling months (Table 1). Aragonite saturation states (Ω_{arag}) in the surface water of the SAB ranged from 2.5 to 4.2. They were lowest close to the coast and increased toward offshore (Fig. 1). Overall, Ω_{arag} showed similar spatial distribution as sea surface salinity (fig. 3 in Jiang et al. 2008), suggesting the importance of low alkalinity and low-calcium water from land in decreasing the carbonate mineral saturation states on the continental shelf (Salisbury et al. 2008).

Seasonally, surface-water Ω_{arag} showed the largest variation on the inner shelf (Fig. 1; Table 1). Area-averaged Ω_{arag} was lowest in March 2005 ($\Omega_{arag} = 2.6$) when the shelf received the most freshwater (Jiang 2009), and highest ($\Omega_{arag} = 3.6$) in July 2005 when sea surface salinity on the shelf was greatest of the year (Jiang et al. 2008). Ω_{arag} on the outer shelf showed little seasonal variation, with area-averaged saturation states being 3.7–4.1 (Table 1).
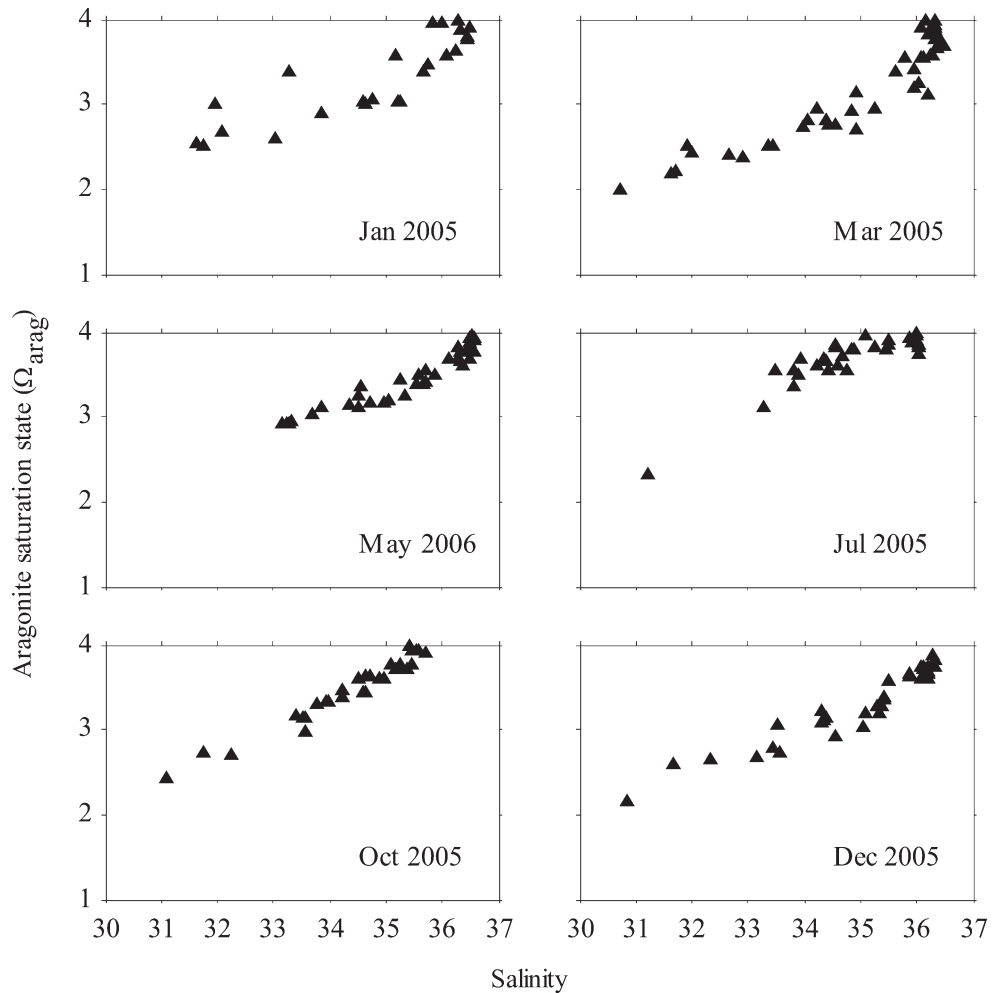
Fig. 3. Plots of aragonite saturation state against salinity on C-transect of the SAB (shoreward shelf break) (Jiang et al. 2008) during all sampling months.

One of the most noticeable features of the vertical distributions of Ω_{arag} is the intrusion of low-saturation-state deep water on the continental slope (Fig. 2). Seaward of the shelf break, Ω_{arag} was $\sim$ 4.0 in the surface water and dropped sharply to 1.0–1.5 at a water depth of 250–600 m. In contrast, Ω_{arag} did not show much vertical variability shoreward of the shelf break, except in July 2005 when upwelled water reached all the way to the outer shelf (Jiang 2009). Ω_{arag} as low as 2.6 was observed at the bottom of the outer shelf in that month.

Calcite saturation state (Ω_{cal}) was approximately 50% higher than Ω_{arag} (Table 1) and showed similar spatial and seasonal variations as Ω_{arag}. For this reason, data for Ω_{cal} were not plotted and the following discussion mainly focuses on Ω_{arag}.

Discussion

Controlling mechanisms—Aragonite saturation states (Ω_{arag}) on the continental shelf of the SAB (shoreward of the shelf break) are strongly affected by the input of low-saturation-state water from land (Fig. 3). Freshwater runoff (small and intermediate rivers) usually has low pH,

high CO_2, and low CO_3^{2-} concentrations (Cai and Wang 1998; Raymond et al. 2000; Borges et al. 2006). Rivers also feature lower calcium concentrations than the oceanic water. The mixing of low-carbonate, low-calcium water from land with high-saturation-state water from the open ocean plays an important role in shaping the carbonate mineral saturation states in the SAB coast.

Plots of Ω_{arag} against salinity (with offshore data included) demonstrate that even though Ω_{arag} on the continental shelf shows a strong linear relationship with salinity, beyond the shelf break it is not the case (Fig. 4a). Instead of forming a straight line, a more complex Ω_{arag} vs. salinity relationship is observed. The L-shaped Ω_{arag} vs. salinity relationship is similar to the temperature–salinity (T-S) plot (Fig. 4b). Correlation analyses show that Ω_{arag} seaward of the shelf break is strongly related to temperature (Fig. 5a). Considering that temperature distribution in this area is a result of mixing (Jiang 2009), we suggest that carbonate mineral saturation states seaward of the shelf break are also controlled by mixing. The L-shaped T-S distribution (Fig. 4b) is due to the three-end-member mixing processes at the shelf break (Jiang 2009). Here, continental shelf water mixes with upwelled low-tempera-
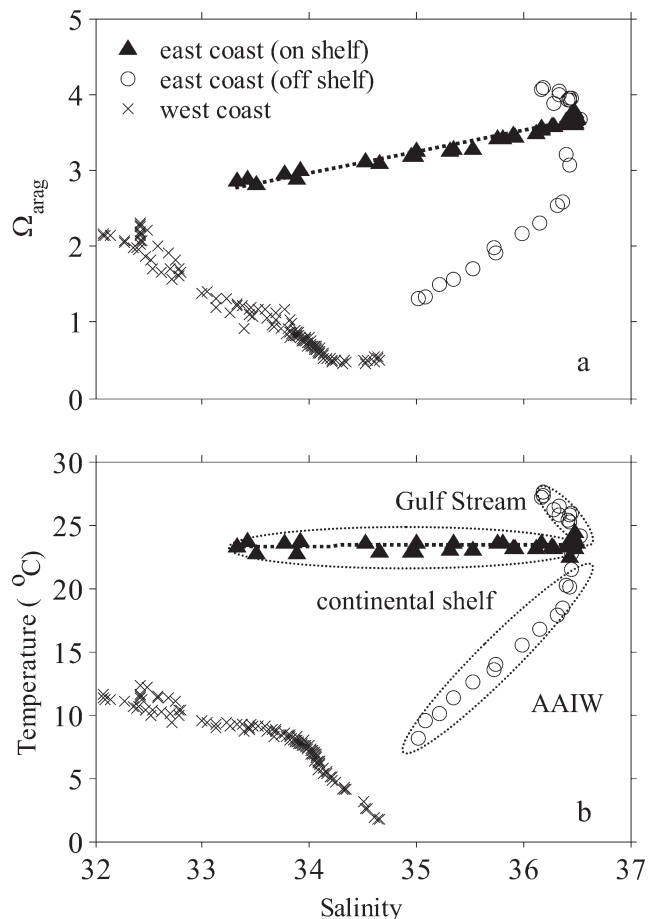
Fig. 4. Plots of (a) aragonite saturation state (Ω_{arag}) against salinity, and (b) temperature against salinity on C-transect of the SAB (Jiang et al. 2008) in May 2006 and on line 5 of the West Coast (Feely et al. 2008) in May 2007.

Fig. 5. Plots of aragonite saturation state (Ω_{arag}) against (a) temperature, and (b) dissolved oxygen (DO) on C-transect of the SAB (Jiang et al. 2008) in May 2006 and on line 5 of the West Coast (Feely et al. 2008) in May 2007.

ture, low-salinity Antarctic intermediate water (AAIW) that is right on the continental slope (Atkinson 1983), and high-temperature, high-salinity Gulf Stream water that is farther away from the slope. The low saturation states of the AAIW are due to the uptake of oxygen and release of carbon dioxide via respiration processes as the water mass transits from the South Atlantic to the study site (Fig. 5b). The upward mixing of the low-saturation-state water from the deeper depths lowers Ω_{arag} of the water mass near the shelf break.

Comparison with the West Coast—Carbonate mineral saturation states in the SAB are much higher than those reported for the West Coast (Feely et al. 2008). Corrosive waters ($\Omega_{arag} < 1$) had been observed in the surface waters off northern California during upwelling in the West Coast (Feely et al. 2008). In contrast, the East Coast was always supersaturated with respect to either aragonite or calcite (Fig. 1). Overall, Ω_{arag} in the SAB (Table 1) is about two units higher than those in the West Coast. Factors contributing to the different carbonate mineral saturation states in the two coasts include: (1) water mass age, (2) water temperature, (3) degree to which the coast experiences upwelling, and (4) influence from freshwater input.
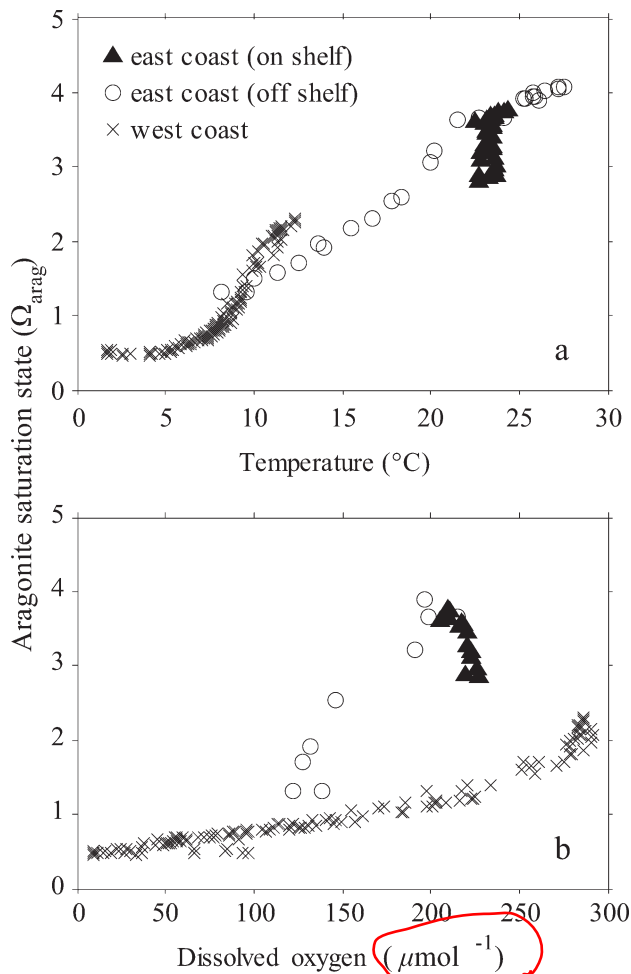
The water mass age is the primary reason why carbonate mineral saturation states in the SAB are so much higher than those in the West Coast. Global oceans circulate like a conveyor belt: Waters sink in the North Atlantic and move southward all the way into the Southern Ocean, then the Pacific Ocean and the Indian Ocean, and get back to the Atlantic Ocean in the surface. During this long journey, organic matter is remineralized, oxygen is consumed, and carbon dioxide is produced. As a result, the older the water is, the lower the carbonate mineral saturation state is. Studies have shown that the oldest waters (with a transit time of about 1000 yr) upwell in the North Pacific (Primeau 2005). In comparison, the deep water in the Atlantic Ocean is much younger.

Water temperature also contributes to the different carbonate mineral saturation states between the two coasts. The West Coast water is up to 10°C colder than the SAB (Fig. 6). Colder source waters are usually more corrosive than warmer waters, mostly due to the increased solubility of CO_2 gas in these waters and partly to the temperature dependences of the solubilities of aragonite and calcite.
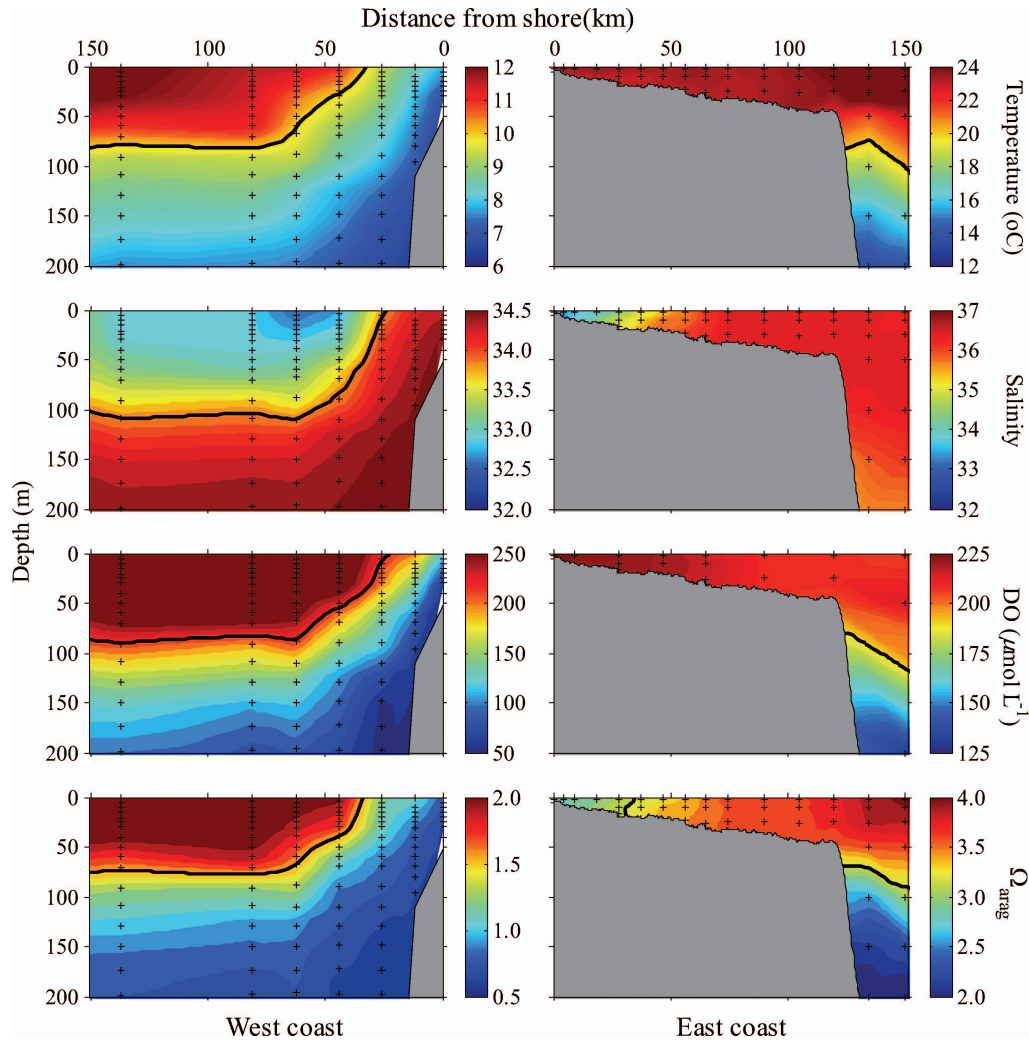
Fig. 6.   Vertical distributions of temperature, salinity, dissolved oxygen (DO), and aragonite saturation state on C-transect of the SAB (Jiang et al. 2008) in May 2006 and on line 5 of the West Coast (Feely et al. 2008) in May 2007.

Another important factor that contributes to the different carbonate mineral saturation states between the two coasts is how they experience upwelling. Deep waters have much lower carbonate mineral saturation states than the surface water because of their older water mass age and increased aragonite and calcite solubilities as a function of the low temperature and high pressure (Feely et al. 2004). Consequently, the degree to which a region experiences upwelling will affect the saturation states in the surface water. The West Coast, which has a narrow continental shelf, is a typical slope-dominated coast (Fig. 6). Here, extensive upwellings of cold subsurface waters occur, caused by the prevailing northwesterly winds acting through the Ekman Effect. In contrast, the East Coast is essentially a wide and shallow continental shelf (Fig. 6) that keeps upwelling off the shelf by strong density front at the shelf break during most times of the year, except in summer when weak subsurface intrusions occur as stratification are combined with upwelling-favorable winds (Atkinson et al. 1984). The sharp contrast in the degree to which the two coasts experience upwelling can be seen from the plots of

aragonite saturation state against salinity, temperature, and DO. In the East Coast, aragonite saturation state showed distinct relationships with salinity (Fig. 4a), temperature (Fig. 5a), and DO (Fig. 5b) for stations on the continental shelf and those beyond the shelf break. In comparison, linear relationships between aragonite saturation state and salinity (Fig. 4a), temperature (Fig. 5a), and DO (Fig. 5b) were seen all across the West Coast.

Both coasts showed lower carbonate mineral saturation states close to the coast than areas farther offshore. However, they are controlled by very different mechanisms. In the West Coast, the low nearshore saturation states are caused by upwelling of low-temperature, high-salinity, low-oxygen, and low-saturation-state deep water (Fig. 6). In contrast, the low saturation states in the nearshore area of the SAB are due to inputs of low-salinity and low-saturation-state freshwater from land (Figs. 3 and 6).

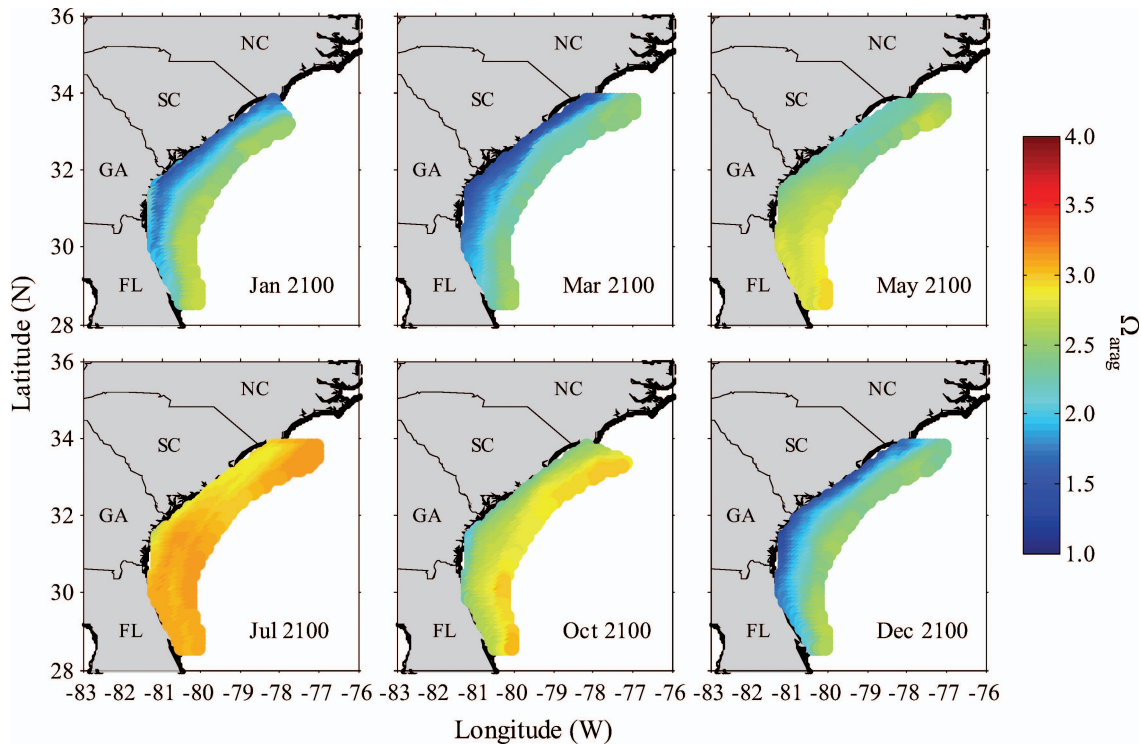*Saturation states in 2100*—Globally, the coastal ocean serves as an important sink of atmospheric CO_2 (Chen and

Fig. 7. Predicted surface water aragonite saturation state in the SAB coast by the year 2100.

Borges 2009). As a result, surface-water pCO_2 in the coastal ocean is rising (Thomas et al. 2007) and the carbonate mineral saturation states are decreasing (Gledhill et al. 2008). Here, aragonite and calcite saturation states in the SAB by the year 2100 were estimated by assuming: (1) sea surface salinity and alkalinity remain invariant; (2) sea surface temperature increases by 2°C; (3) atmospheric CO_2 concentration increases to a value of 800 μmol mol^{-1} (according to the IPCC B1 emission scenario).

The B1 scenario provides one of the most conservative estimates of the cumulative carbon dioxide emissions by the year 2100 (Nakićenović and Swart 2000). It describes "a world with the global population peaking in midcentury and declining thereafter; the economy is moving toward a service and information economy, with reductions in material intensity, and the introduction of clean and resource-efficient technologies." Therefore, the calculation for this study provides a lower-end estimate of the changes in carbonate mineral saturation states.

Results show that by the end of this century, saturation states of aragonite and calcite will decrease by ~ 20–40% (Table 1 and Fig. 7). The largest drop (35–40%) occurs in winter, when the difference between the modern sea surface pCO_2 level and that of 2100 is the largest, and the smallest change (17–20%) occurs in summer on the inner shelf, where the sea surface pCO_2 is already very high (Jiang et al. 2008). Ω_{arag} as low as 1.3 will be seen on the inner shelf of the SAB during spring, although the outer shelf will continue to be supersaturated, with Ω_{arag} ranging from 2.3 to 3.1. Ω_{cal} will remain above 2 all across the SAB even by the year 2100 (Table 1).

Calcareous organisms usually require seawater Ω-values much higher than 1 to achieve optimal growth. Even though the carbonate mineral saturation states in this region will continue to be supersaturated by the end of this century, such a dramatic drop in saturation states could lead to reduced calcification and juvenile survival rates. In addition, as bottom water and water in surface sediments usually have lower pH than the surface water, such changes will threaten the health of bottom- or benthic-dwelling organisms with carbonate shells, such as the abundant and diverse communities living in the Gray Reef National Marine Sanctuary in the SAB shelf.

The decline rates of carbonate mineral saturation state of this study are close to those of the global ocean, as predicted by ocean circulation models (Cao et al. 2007; McNeil and Matear 2007). However, one needs to keep in mind that the above calculation of carbonate mineral saturation states in 2100 is solely based on long-term changes in atmospheric CO_2 (of one emission scenario). In the coastal ocean, other processes, such as primary production, respiration, nitrification, denitrification, and sulfate reduction, could exert a larger control on carbonate mineral saturation state (Borges and Gypens 2010; Feely et al. 2010). Although long-term monitoring is lacking, an 8-yr time-series study from a coastal site off Washington, USA shows that the decrease of pH and carbonate mineral saturation state in the coastal ocean is, in some cases, much faster than that in the open ocean (Wooton et al. 2008). These rapid changes are probably the result of several of these processes working together to rapidly reduce the pH, as suggested by Feely et al (2010).

References

ATKINSON, L. P. 1983. Distribution of Antarctic intermediate water over the Blake Plateau. J. Geophys. Res. **88:** 4699–4704, doi:10.1029/JC088iC08p04699

———, P. G. O'MALLEY, J. A. YODER, AND G.-A. PAFFENHÖFFER. 1984. The effect of summertime shelf break upwelling on nutrient flux in southeastern United States continental shelf waters. J. Mar. Res. **42:** 969–993, doi:10.1357/002224084788520756

BORGES, A. V., AND N. GYPENS. 2010. Carbonate chemistry in the coastal zone responds more strongly to eutrophication than ocean acidification. Limnol. Oceanogr. **55:** 346–353.

———, L.-S. SCHIETTECATTE, G. ABRIL, B. DELILLE, AND F. GAZEAU. 2006. Carbon dioxide in European coastal waters. Est. Coast. Shelf Sci. **70:** 375–387, doi:10.1016/j.ecss.2006.05.046

BREWER, P. G., AND K. C. HESTER. 2009. Ocean acidification and the increasing transparency of the ocean to low-frequency sound. Oceanography **22:** 86–93.

BROECKER, W. S. 2003. The oceanic $CaCO_3$ cycle, p. 529–549. *In* H. Elderfield [ed.], The oceans and marine geochemistry, treatise on geochemistry. Elsevier.

CAI, W.-J., AND Y. WANG. 1998. The chemistry, fluxes, and sources of carbon dioxide in the estuarine waters of the Satilla and Altamaha Rivers, Georgia. Limnol. Oceanogr. **43:** 657–668, doi:10.4319/lo.1998.43.4.0657

CALDEIRA, K., AND E. WICKETT. 2003. Anthropogenic carbon and ocean pH. Nature **425:** 365, doi:10.1038/425365a

CAO, L., K. CALDEIRA, AND A. K. JAIN. 2007. Effects of carbon dioxide and climate change on ocean acidification and carbonate mineral saturation. Geophys. Res. Lett. **34:** L05607, doi:10.1029/2006GL028605

CHEN, C.-T. A., AND A. V. BORGES. 2009. Reconciling opposing views on carbon cycling in the coastal ocean: Continental shelves as sinks and near-shore ecosystems as sources of atmospheric CO_2. Deep-Sea Res. II **56:** 578–590, doi:10.1016/j.dsr2.2009.01.001

CLAYTON, T., AND R. H. BRYNE. 1993. Spectrophotometric seawater pH measurements: Total hydrogen ion concentration scale calibration of *m*-cresol purple and at-sea results. Deep-Sea Res. I **40:** 2115–2129, doi:10.1016/0967-0637(93)90048-8

DICKSON, A. G. 1990. Standard potential of the reaction: AgCl(s) + 1/2 H_2(g) = Ag(s) + HCl(aq), and the standard acidity constant of the ion HSO_4^- in synthetic seawater from 273.15 to 318.15K. J. Chem. Thermodyn. **22:** 113–127, doi:10.1016/0021-9614(90)90074-Z

———, AND F. J. MILLERO. 1987. A comparison of the equilibrium constants for the dissociation of carbonic acid in seawater media. Deep-Sea Res. **34:** 1733–1743.

DONEY, S. C., W. M. BALCH, V. J. FABRY, AND R. A. FEELY. 2009*a*. Ocean acidification: A critical emerging problem for the ocean sciences. Oceanography **22:** 18–27.

———, V. J. FABRY, R. A. FEELY, AND J. A. KLEYPAS. 2009*b*. Ocean acidification: The other CO_2 problem. Ann. Rev. Mar. Sci. **1:** 169–192, doi:10.1146/annurev.marine.010908.163834

FABRY, V. J. 2008. Marine calcifers in a high-CO_2 ocean. Science **320:** 1020–1022, doi:10.1126/science.1157130

FEELY, R. A., S. C. DONEY, AND S. R. COOLEY. 2009. Ocean acidification: Present conditions and future changes in a high-CO_2 world. Oceanography **22:** 36–47.

———, C. L. SABINE, J. M. HERNANDEZ-AYON, D. LANSON, AND B. HALES. 2008. Evidence for upwelling of corrosive acidified water onto the continental shelf. Science **320:** 1490–1492, doi:10.1126/science.1155676

———, ———, K. LEE, W. BERELSON, J. KLEYPAS, V. J. FABRY, AND F. J. MILLERO. 2004. Impact of anthropogenic CO_2 on the $CaCO_3$ system in the oceans. Science **305:** 362–366, doi:10.1126/science.1097329

———, AND OTHERS. 2010. The combined effects of ocean acidification, mixing, and respiration on pH and carbonate saturation in an urbanized estuary. Estuar. Coast. Shelf Sci. **88:** 442–449, doi:10.1016/j.ecss.2010.05.004

GLEDHILL, D. K., R. WANNINKHOF, F. J. MILLERO, AND M. EAKIN. 2008. Ocean acidification of the Greater Caribbean Region 1996–2006. J. Geophys. Res. **113:** C10031, doi:10.1029/2007JC004629

HÖNISCH, B., N. G. HEMMING, D. ARCHER, M. SIDDALL, AND F. MCMANUS. 2009. Atmospheric carbon dioxide concentration across the mid-Pleistocene transition. Science **324:** 1551–1554, doi:10.1126/science.1171477

HUTCHINS, D., M. R. MULHOLLAND, AND F. FU. 2009. Nutrient cycles and marine microbes in a CO_2-enriched ocean. Oceanography **22:** 128–145.

JIANG, L.-Q. 2009. Biogeochemical cycling of carbon dioxide in estuaries and the continental shelf of the southeastern United States. Ph.D. thesis. Univ. of Georgia.

———, W.-J. CAI, R. WANNINKHOF, Y. WANG, AND H. LÜGER. 2008. Air–sea CO_2 fluxes on the U.S. South Atlantic Bight: Spatial and seasonal variability. J. Geophys. Res. **113:** C07019, doi:10.1029/2007JC004366

KLEYPAS, J. A., R. W. BUDDEMEIER, D. ARCHER, J.-P. GATTUSO, C. LANGDON, AND B. N. OPDYKE. 1999. Geochemical consequences of increased atmospheric carbon dioxide on coral reefs. Science **284:** 118–120, doi:10.1126/science.284.5411.118

———, R. A. FEELY, V. J. FABRY, C. LANGDON, C. L. SABINE, AND L. L. ROBBINS. 2006. Impacts of ocean acidification on coral reefs and other marine calcifiers: A guide to future research. Report of a workshop held 18–20 April 2005, St. Petersburg, FL, sponsored by NSF, NOAA, and the U.S. Geological Survey.

LE QUÉRÉ, C., AND OTHERS. 2009. Trends in the sources and sinks of carbon dioxide. Nature Geosci. **2:** 831–836, doi:10.1038/ngeo1689

LEWIS, E., AND D. W. R. WALLACE. 1998. Program developed for CO_2 system calculations, ORNL/CDIAC-105. Carbon Dioxide Information Analysis Center, Oak Ridge National Laboratory, U.S. Department of Energy, Oak Ridge, Tennessee.

MARLAND, G., T. A. BODEN, AND R. J. ANDRES. 2009. Global, regional, and national fossil-fuel CO_2 emissions. Carbon Dioxide Information Analysis Center, Oak Ridge National Laboratory, U.S. Department of Energy, Oak Ridge, Tennessee.

MCNEIL, B. I., AND R. J. MATEAR. 2007. Climate change feedbacks on future oceanic acidification. Tellus **59B:** 191–198.

MEHRBACH, C., C. H. CULBERSON, J. E. HAWLEY, AND R. N. PYTKOWICZ. 1973. Measurement of the apparent dissociation constants of carbonic acid in seawater at atmospheric pressure. Limnol. Oceanogr. **18:** 897–907, doi:10.4319/lo.1973.18.6.0897

MILLERO, F. J., R. WOOSLEY, B. DITROLIO, AND J. WATERS. 2009. Effect of ocean acidification on the speciation of metals in seawater. Oceanography **22:** 72–85.

MUCCI, A. 1983. The solubility of calcite and aragonite in seawater at various salinities, temperatures, and one atmosphere total pressure. Am. J. Sci. **283:** 781–799.

NAKIĆENOVIĆ, N., AND R. SWART. 2000. Special report on emissions scenarios-The third assessment report of the Intergovernmental Panel on Climate Change. Cambridge Univ. Press.

ORR, J. C., AND OTHERS. 2005. Anthropogenic ocean acidification over the twenty-first century and its impact on calcifying organisms. Nature **437:** 681–686, doi:10.1038/nature04095

PAI, S.-C., G.-C. GONG, AND K.-K. LIU. 1993. Determination of dissolved oxygen in seawater by direct spectrophotometry of total iodine. Mar. Chem. **41:** 343–351, doi:10.1016/0304-4203(93)90266-Q

PRIMEAU, F. 2005. Characterizing transport between the surface mixed layer and the ocean interior with a forward and adjoint global ocean transport model. J. Phys. Oceanogr. **35:** 545–564, doi:10.1175/JPO2699.1

RAYMOND, P. A., J. E. BAUER, AND J. J. COLE. 2000. Atmospheric CO_2 evasion, dissolved inorganic carbon production, and net heterotrophy in the York River estuary. Limnol. Oceanogr. **45:** 1707–1717, doi:10.4319/lo.2000.45.8.1707

RIES, J. B., A. L. COHEN, AND D. C. MCCORKLE. 2009. Marine calcifiers exhibit mixed responses to CO_2-induced ocean acidification. Geology **37:** 1057–1152.

RILEY, J. P., AND M. TONGUDAI. 1967. The major cation/chlorinity ratios in sea water. Chem. Geol. **2:** 263–269, doi:10.1016/0009-2541(67)90026-5

SALISBURY, J., M. GREEN, C. HUNT, AND J. CAMPBELL. 2008. Coastal acidification by rivers: A threat to shellfish? EOS: Trans. Am. Geophys. Union **89:** 513–528, doi:10.1029/2008EO500001

THOMAS, H., AND OTHERS. 2007. Rapid decline of the CO_2 buffering capacity in the North Sea and implications for the North Atlantic Ocean. Global Biogeochem. Cycles **21:** GB4001, doi:10.1029/2006GB002825

VAN HEUVEN, S., D. PIERROT, E. LEWIS, AND D. W. R. WALLACE. 2009. Matlab program developed for CO_2 system calculations (http://cdiac.ornl.gov/oceans/co2rprt.html). Carbon Dioxide Information Analysis Center, Oak Ridge National Laboratory, U.S. Department of Energy, Oak Ridge, Tennessee.

WOLF-GLADROW, D. A., U. RIEBESELL, S. BURKHARDT, AND J. BIJMA. 1999. Direct effects of CO_2 concentration on growth and isotopic composition of marine plankton. Tellus **51B:** 461–476.

WOOTTON, J. T., C. A. PFISTER, AND J. D. FORESTER. 2008. Dynamic patterns and ecological impacts of declining ocean pH in a high-resolution multiyear data set. Proc. Natl. Acad. Sci. USA **105:** 18848–18853, doi:10.1073/pnas.0810079105